JOURNAL OF RAMAN SPECTROSCOPY, VOL. 18, 345-349 (1987)

UV Resonance Raman Excitation Profiles of *l*-Cystine

Craig R. Johnson and Sanford A. Asher*
Department of Chemistry, University of Pittsburgh, Pittsburgh, Pennsylvania 15260, USA

The UV Raman excitation profiles of *l*-cystine have been measured between 220 and 514.5 nm. No enhancement is observed from the lowest energy electronic transition ($\lambda_{max} = 245$ nm). The excitation profiles for the S–S, C–S and C=O stretching vibrations are each satisfactorily modeled by standard Albrecht *A*-term pre-resonance expressions which indicate that the Raman intensities derive from a state(s) at *ca* 170 nm which is probably $\sigma \rightarrow \sigma^*$ in character. Selective enhancement of disulfide stretching vibrations in proteins will require excitation in the vacuum UV spectral region.

INTRODUCTION

Disulfide bonds uniquely control and determine protein secondary structure. Raman spectroscopy has provided a unique probe of disulfide bond conformation in both small peptides and proteins.[1-3] The S–S stretch which occurs between 500 and 550 cm^{-1} in the Raman spectra monitors the geometry about the disulfide bond and is sensitive to the relative orientation of the groups bonded to the sulfur atoms.[4,5] The Raman band due to the S–S stretching vibration often dominates the low-frequency Raman spectra of proteins obtained with visible excitation wavelengths. The S–S stretching vibrational frequencies, and also the amide vibrational frequencies and intensities, are routinely used to study protein conformation.[1-3] Recently, it was demonstrated that aromatic amino acids in proteins can be probed by using ultraviolet excitation within the absorption bands of phenylalanine, tyrosine and tryptophan residues.[6,7] The UV resonance Raman enhancement of the aromatic amino acids permits studies of these residues in proteins at sub-millimolar concentrations. Much higher concentrations and amounts of protein are required with visible excitation. The disulfide bond is a major contributor to protein UV absorption below 240 nm.

This study was undertaken in order to determine whether ultraviolet resonance Raman (UVRR) spectroscopy could be used to study selectively the disulfide linkages in proteins. *l*-Cystine was chosen as a simple model for the disulfide bond of proteins. The UVRR excitation profiles of *l*-cystine above 220 nm show little resonance enhancement of S–S or C–S Raman scattering. Resonance enhancement of the disulfide group will require excitation in the vacuum UV region.

EXPERIMENTAL

l-Cystine was obtained from Sigma Chemical Company and used without further purification. All *l*-cystine solutions were prepared in 1 M HCl (Fisher). Sodium perchlorate (0.2 M) was used as an internal intensity standard.[8] The instrumentation and methods used to obtain the UVRR spectra have been described in detail elsewhere.[9] To avoid photodamage, the sample solutions were circulated through the laser beam in a quartz capillary. Care was taken to avoid tight focusing of the laser beam within the sample. Previous studies in this laboratory have shown that production of phototransients or optical saturation at high power densities can be serious impediments to measurements of both absolute and relative Raman cross-sections.[6b,10] The Raman spectrum of *l*-cystine was studied as a function of incident laser power at 310 nm excitation to ensure that no photochemical or saturation phenomena were present. Spectra were obtained with powers ranging from 7 to 70 mW. The intensity ratios of the $\nu_{(S-S)}$ and $\nu_{(C-S)}$ bands of *l*-cystine to the 932 cm^{-1} ClO_4^- band were constant, within experimental error, over this range of powers. At the higher powers, however, a new Raman band at 530 cm^{-1} appeared as a shoulder on the $\nu_{(S-S)}$ band of *l*-cystine. Electronic absorption spectra of the *l*-cystine solutions before and after laser irradiation showed less than a 5% change in the absorption. That some photochemistry occurred was evidenced by a sulfurous odor from the samples.

Relative intensity ratios were determined from peak-height measurements of the Raman bands. The intensity ratios were corrected for monochromator and detector efficiencies. The *l*-cystine Raman intensities were referenced to the 932 cm^{-1} band of ClO_4^- (0.2 M). Total differential Raman scattering cross-sections for the *l*-cystine bands were determined from the relative ratio measurement methods described previously.[11] The Raman frequencies quoted are estimated to be accurate to ± 5 cm^{-1}.

Raman spectra at excitation wavelengths longer than 245 nm were obtained by collecting the Raman scattering at 90° to the incident laser beam. Owing to small resonance enhancement and to attenuation of the Raman scattering by self-absorption, the data for excitation wavelengths shorter than 245 nm were obtained by using a 135° backscattering geometry. Spectra with acceptable signal-to-noise ratios could not be obtained at these wavelengths with 90° scattering. Both the incident laser beam and the Raman scattering are attenuated by *l*-cystine absorption (self-absorption). For Raman

* Author to whom correspondence should be adressed.

0377-0486/87/050345-05 $05.00

Received 16 July 1986
Accepted 4 August 1986

measurements the net Raman scattered intensity depends on the laser intensity, the Raman cross-section and the absorption cross-section. Samples with low Raman cross-sections require high concentrations. As resonance is approached, the absorption cross-section increases. If the absorption cross-section increases faster than the Raman cross-section the net Raman scattering intensity can decrease below the detection limit for the spectrometer. This phenomenon often occurs for Raman experiments in resonance with absorption bands of relatively low molar absorptivity. An example was recently encountered in studies of $(CN)_5Fe(imidazole)^{2-}$, which has low cross-sections for both absorption and Raman scattering.[12] A more quantitative discussion of the relationship between measured Raman intensities and Raman and absorption cross-sections will be given in more detail elsewhere.[13]

Measurements of the Rayleigh scattering from the *l*-cystine solutions and from solutions containing just the perchlorate standard were made by using a series of neutral density filters and quartz plates to attenuate the incident laser beam. This experimental arrangement was described in detail elsewhere.[8] As in the Raman measurements, the Rayleigh scattering was measured relative to the 932 cm^{-1} Raman band of perchlorate.

Depolarization ratio measurements were made by using a Polacoat analyzer.

RESULTS AND DISCUSSION

Figure 1 shows the Raman spectrum of *l*-cystine obtained with 488 nm excitation. Previous workers have tentatively assigned many of the Raman bands observed.[14] The two most intense bands at 503 and 665 cm^{-1} have been assigned to the S–S stretching vibration [$\nu_{(S-S)}$] and the C–S stretching vibration [$\nu_{(C-S)}$], respectively. The $\nu_{(S-S)}$ band in protein spectra is diagnostic of the bonding geometry about the disulfide linkage. The $\nu_{(C-S)}$ band in protein spectra can derive from either *l*-cystine, *l*-cysteine or *l*-methionine residues and is, therefore, less readily useful for characterizing disulfide bonding in proteins. The band at 1735 cm^{-1} is assigned to C=O stretching vibrations. The broad band at *ca* 1640 cm^{-1} derives from water. The other Raman bands observed are weak relative to the S–S and S–C stretching vibrations and are primarily due to C–C, C–O and C–H single-bond bending and/or stretching vibrations. These Raman bands remain weak for all excitation wavelengths used in this work. Only the $\nu_{(S-S)}$, $\nu_{(C-S)}$ and $\nu_{(C=O)}$ bands were studied in detail.

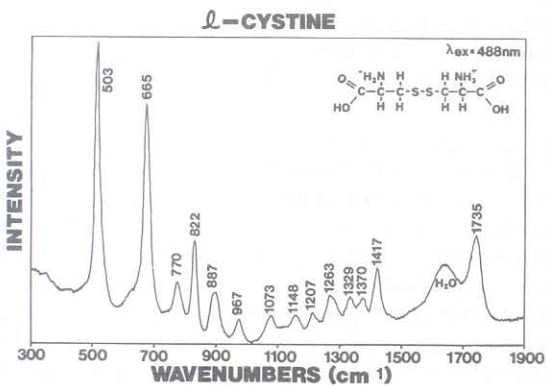

Figure 1. Normal Raman spectrum of an aqueous 0.5 M *l*-cystine solution (1 M in HCl) obtained with 488 nm excitation (Ar^+ laser).

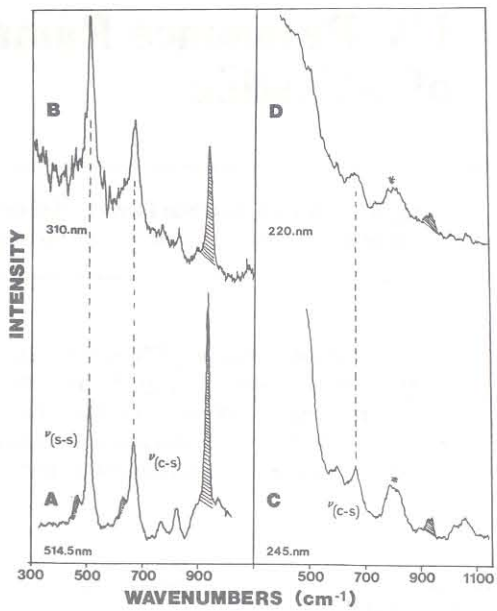

Figure 2. Raman spectra of *l*-cystine at several excitation wavelengths. (A) λ_{ex}=514.5 nm, 265 mW average power (CW Ar^+ laser), spectral bandpass=5 cm^{-1}, [*l*-cys]=0.25 M; (B) λ_{ex}=310 nm, 3.5 mW average power, spectral bandpass=15 cm^{-1}, [*l*-cys]=0.25 M; (C) λ_{ex}=245 nm, 2 mW average power, spectral bandpass=20 cm^{-1}, [*l*-cys]=0.1 M; (D) λ_{ex}=220 nm, 5 mW average power, spectral bandpass=30 cm^{-1} [*l*-cys]=0.05 M. Spectra B, C and D were obtained with an Nd–YAG laser operated at 20 Hz. Each solution was prepared in 1 M HCl and contained 0.2 M $NaClO_4$. The ClO_4^- Raman bands are shaded. Spectra A and B were obtained using 90° scattering and spectra C and D were obtained using 135° backscattering. The broad feature indicated by the asterisks in spectra C and D derives from Raman scattering from the quartz capillary.

Raman spectra of *l*-cystine at several excitation wavelengths are shown in Fig. 2. As seen in Fig. 2A, the Raman bands of ClO_4^- slightly overlap several bands of *l*-cystine. The 932 cm^{-1} band of ClO_4^- is bracketed by the 887 and 967 cm^{-1} bands of *l*-cystine. Because neither of these *l*-cystine bands is very intense for any excitation wavelength used, they do not interfere with the peak-height measurement of ClO_4^-, the internal standard. The ClO_4^- bands at 462 and 628 cm^{-1} are weak compared with the $\nu_{(S-S)}$ and $\nu_{(C-S)}$ vibrations in all spectra and do not seriously interfere with the peak-height measurements of the *l*-cystine bands. The resonance (pre-resonance) Raman spectrum in Fig. 2B was obtained at an excitation wavelength of 310 nm, where *l*-cystine just begins to absorb. Figure 3 shows the absorption spectrum of *l*-cystine and displays one rather weak, broad, featureless band in the UV region at *ca* 245 nm, with a molar absorptivity[15] of 300 l mol^{-1} cm^{-1}. This absorption band is a shoulder on a much stronger transition which has its absorption maximum in the vacuum UV region. The 310 nm UV Raman spectrum shows that the $\nu_{(S-S)}$ and $\nu_{(C-S)}$ bands of *l*-cystine are enhanced relative to ClO_4^- as the excitation wavelength is decreased.

Resonance Raman spectra of *l*-cystine obtained at 245 and 220 nm excitation are shown in Fig. 2C and D. As can be seen, the 503 cm^{-1} $\nu_{(S-S)}$ band could not be

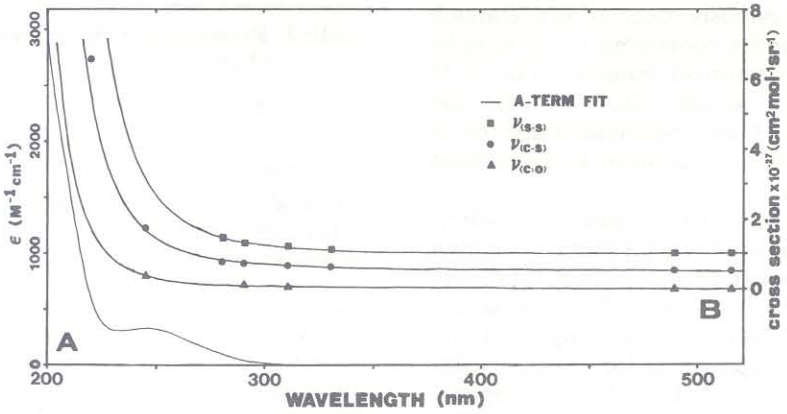

Figure 3. Albrecht *A*-term fits for the *l*-cystine Raman scattering cross-section data. (A) UV–visible electronic absorption spectrum of *l*-cystine; (B) Raman excitation profiles of *l*-cystine. The solid lines were calculated with the Albrecht *A*-term parameters shown in Table 1. *For clarity, the data for* $\nu_{(C-S)}$ *and* $\nu_{(S-S)}$ *are offset along the ordinate by* ±0.5 *and* ±1 *cross-section units, respectively.*

resolved in these spectra owing to interferences in the low-frequency region from stray light from Rayleigh scattering. Discrimination against Rayleigh scattering becomes more difficult as excitation occurs further in the UV (given the same instrumental parameters) because of the decrease in the energy dispersion of the spectrograph. The spectrograph dispersion is linear in wavelength.

The increased stray light interference may also derive from an increase in elastic scattering due to resonance enhancement of the Rayleigh scattering. Simple Raman theory predicts that the magnitude of resonance enhancement of a symmetric fundamental mode is related to the displacement of the excited state along that normal coordinate. A large displacement along a normal coordinate results in a large resonance enhancement of the Raman scattering. Conversely, the magnitude of resonance Rayleigh enhancement is inversely related to the geometric displacement of the resonant excited state along a symmetric normal coordinate.

We attempted to measure the wavelength dependence of the resonance Rayleigh scattering in order to determine directly if the paucity of resonance Raman enhancement was due to a lack of expansion of the S—S bond in the 245 nm electronic transition. Several measurements were made to determine the magnitude of the resonance Rayleigh enhancement for *l*-cystine. At 245 nm (in resonance) the Rayleigh scattering from the *l*-cystine solution is *ca* 14 times more intense than that of an aqueous solution of perchlorate. At 620 nm excitation, far from resonance, similar Rayleigh scattering is observed from the *l*-cystine and perchlorate solutions. Although resonance Rayleigh experiments can be fraught with experimental artifacts, it appears from these results that significantly more resonance Rayleigh than resonance Raman enhancement occurs for *l*-cystine solutions with UV excitation.

The excitation profiles of the $\nu_{(S-S)}$, $\nu_{(C-S)}$ and $\nu_{(C=O)}$ vibrations of *l*-cystine are shown in Fig. 3. No enhancement from the 245 nm absorption band is evident from the profiles. Thus, the Raman intensity derives from a state or states at higher energy. The energy of the state from which the Raman intensity derives was determined by fitting the excitation profile data to an Albrecht *A*-term expression:

$$\sigma_R = K\nu_0(\nu_0 - \nu_R)^3 \left[\frac{\nu_e^2 + \nu_{20}}{(\nu_e^2 - \nu_0^2)^2}\right]^2$$

where σ_R is the cross-section of Raman mode R. K is a constant independent of excitation energy and is related to the oscillator strength of the electronic transition from which the Raman intensity derives and the coupling between mode R and the electronic transition, ν_0 is the laser energy (cm^{-1}), ν_R is the Raman frequency of the mode (cm^{-1}) and ν_e is the transition frequency to the pre-resonant electronic excited state (cm^{-1}).

The results of the *A*-term fits are shown in Table 1 and the fit is indicated by the solid curves in Fig. 3. The estimated errors in the experimental cross-sections are ±10% for the data between 280 and 514.5 nm and ±20% for the data between 245 and 220 nm. The *A*-term fits appear to be satisfactory considering the standard deviations of the measured data. All three Raman bands studied appear to derive their intensity from an electric transition near 170 nm.

The lowest energy disulfide absorption band (245 nm) has been assigned to an $n \rightarrow \sigma^*$ (or $n^* \rightarrow \sigma^*$) transition localized on the disulfide functional group.[15,16] Excited-state calculations of the electronic spectrum of dimethyl disulfide predict an allowed disulfide $\sigma \rightarrow \sigma^*$ transition at *ca* 180 nm (depending on dihedral angle).[16] The 170 nm transition of *l*-cystine located by the excitation profile data may be reasonably assigned to this transition. The $\nu_{(C=O)}$ mode derives intensity from a transition at similar energy. The $\nu_{(C=O)}$ stretching mode could derive intensity from a $\pi \rightarrow \pi^*$ (C=O) transition or from a $\sigma \rightarrow \sigma^*$ transition within the C—O framework. Enhancements from a *ca* 180 nm

Table 1. Albrecht *A*-term fits to the *l*-cystine excitation profiles

Mode	Wavenumbers (cm^{-1})	$\nu_e \times 10^3$ (cm^{-1})	Wavelength (nm)	$K \times 10^{-28}$ (cm^{-1} molecule^{-1} sr^{-1})
$\nu_{(S-S)}$	503	58.9	170	3.16
$\nu_{(C-S)}$	665	60.3	166	2.28
$\nu_{(C=O)}$	1735	59.0	170	0.57

$\pi \rightarrow \pi^*$ transition was previously observed in acetamide for amide vibrational modes containing C=O stretching.[11] Hence the 170 nm resonant transition for C=O vibrational enhancement could either indicate the existence of an additional C=O electronic transition or suggest that the 170 nm S-S transition is delocalized throughout the molecule.

Depolarization ratios for the $\nu_{(S-S)}$ and $\nu_{(C-S)}$ vibrations were measured at 514.5 and 310 nm excitation wavelengths. The measured depolarization ratios are 0.14 ± 0.05 (0.22 ± 0.05) at 514.5 and 0.32 ± 0.05 (0.32 ± 0.05) at 310 nm for the S-S (C-S) stretching vibration. The value of the depolarization ratio for 310 nm excitation approaches that expected (0.33) if one diagonal tensor element dominates the Raman scattering. This would occur if one polarized electronic transition dominated the scattering intensity. This is consistent with the behavior expected as resonance excitation approaches a $\sigma \rightarrow \sigma^*$ transition localized on the disulfide bond. The transitions would be strongly polarized along the S—S bond axis.

The results presented here have important implications for future UVRR studies of proteins. The lack of significant resonance enhancement of the $\nu^{(S-S)}$mode in the UV region at wavelengths greater than 220 nm indicates that it will be difficult to detect this mode in proteins for excitation in this spectral region. Indeed, recent UVRR spectra of lysozyme[6b] and insulin[17] show no enhancement for C-S or S-S vibrations. The aromatic amino acids have higher Raman cross-sections, as shown in Table 2; however, disulfide bonding in proteins is easily studied using visible excitation wavelengths. Our results indicate that it should also be possible to enhance these vibrations selectively with excitation in the vacuum UV spectral region at *ca* 170 nm.

The selectivity available for UVRR (250–220 nm) for particular amino acid residues is illustrated in Table 2. With visible excitation (488 nm) all of the chromophores studied have similar cross-sections and each of them have previously been identified in the normal Raman spectra of proteins.[1-3] Tyrosinate and tryptophan have the lowest cross-sections with visible wavelength excitation, while *l*-cystine (disulfide bond) has the largest cross-section. Peptide bond vibrations usually dominate the normal Raman spectra of proteins owing to the large numbers of these moeities in the protein. With UV excitation (220 nm) these peptide bond vibrations are the weakest scatters, while the tyrosine and tryptophan residues scatter 50–125 times better than disulfide vibrations. All of the major bands observed in the UVRR spectra of proteins can be assigned to tyrosine, tryptophan or phenylalanine. No interference from the weaker scatterers—histidine, disulfide bonds and peptide bonds—are observed.[6]

Table 2. Raman Scattering cross-sections for UV chromophores of proteins

Chromophore	Mode (cm^{-1})[a]	Cross-section $\times 10^{-30}$ (cm^2 molecule^{-1} sr^{-1}) λ_{ex}=488.0 nm	Cross-section $\times 10^{-30}$ (cm^2 molecule^{-1} sr^{-1}) λ_{ex}=220.0 nm
l-Cystine[b] (disulfide bond)	503	6.1	6080
N-Methylacetamide[c] (peptide bond)	1316	3	3900
Phenylalanine[d]	1604	3.8	176000
Tryptophan[d]	1006	1.6	>830000[g]
Tyrosine[e]	1609	—	353000
Tyrosinate[d]	1601	1.3	141000
Imidazole[f]	1430	8	67600

[a] A representative mode, generally one of high relative intensity with UV excitation, was chosen
[b] This work.
[c] Ref. 11.
[d] Ref. 6b.
[e] Ref. 18.
[f] Ref. 19.
[g] Owing to saturation effects, this number represents a lower limit.

Acknowledgements

We gratefully acknowledge partial support of this work from the NIH, grant IRO1GM30741-04. Sanford A. Asher is an Established Investigator of the American Heart Association; this work was carried out during the tenure of an Established Investigatorship of the American Heart Association and with funds contributed in part by the American Heart Association, Pennsylvania affiliate.

REFERENCES

1. P. R. Carey, *Biochemical Applications of Raman and Resonance Raman Spectroscopies*, pp. 88 and 97. Academic Press, New York (1982).
2. A. T. Tu, *Raman Spectroscopy in Biology: Principles and Applications*, pp. 91–94. Wiley, New York (1982).
3. F. S. Parker, *Applications of Infrared, Raman and Resonance Raman Spectroscopy in Biochemistry*, pp. 93–100. Plenum Press, New York (1983).
4. H. E. Van Wart, A. Lewis, H. A. Scheraga and F. D. Saeva, *Proc. Natl. Acad. Sci. USA* **70**, 2619 (1973); F. R. Maxfield and H. A. Scheraga, *Biochemistry* **16**, 4443 (1977); H. E. Van Wart, H. A. Scheraga and R. B. Martin, *J. Phys. Chem.* **80**, 1832 (1976); H. E. Van Wart and H. A. Scheraga, *J. Phys. Chem.* **80**, 1812, 1823 (1976).
5. H. Sugeta, A. Go and T. Miyazawa, *Chem. Lett.* 83 (1972); H. Sugeta, A. Go and T. Miyazawa, *Bull. Chem. Soc. Jpn.* **46**, 3407 (1973).
6. (a) C. R. Johnson, M. Ludwig, S. E. O'Donnell and S. A. Asher, *J. Am. Chem. Soc.* **106**, 5008 (1984); (b) S. A. Asher, M. Ludwig and C. R. Johnson, *J. Am. Chem. Soc.* **108**, 3186 (1986); (c) I. Harada and H. Takeuchi in *Advances in Spectroscopy: Biological Systems*, edited by R. J. H. Clark and R. E. Hester, in press. Wiley, New York.
7. R. P. Rava and T. G. Spiro, *J. Phys. Chem.* **89**, 1856 (1985); R. P. Rava and T. G. Spiro, *J. Am. Chem. Soc.* **106**, 4062 (1984).
8. J. M. Dudik, C. R. Johnson and S. A. Asher, *J. Chem. Phys.* **82**, 1732 (1985).
9. S. A. Asher, C. R. Johnson and J. Murtaugh, *Rev. Sci. Instrum.* **54**, 1657 (1983); C. M. Jones, T. A. Naim, M. Ludwig, J. Murtaugh, P. R. Flaugh, J. M. Dudik, C. R. Johnson and S. A. Asher, *Trends Anal. Chem.* **4**, 75 (1985).
10. C. R. Johnson, M. Ludwig and S. A. Asher, *J. Am. Chem. Soc.* **108**, 905 (1986).
11. J. M. Dudik, C. R. Johnson and S. A. Asher, *J. Phys. Chem.* **89**, 3805 (1985).
12. C. M. Jones, C. R. Johnson, S. A. Asher and R. E. Shepherd, *J. Am. Chem. Soc.* **107**, 3772 (1985).
13. S. A. Asher, in preparation.

14. L. Simons, G. Bergström, G. Blomfelt, S. Forss, H. Stenbäck and G. Wansen, *Commentat. Phys. Math. Soc. Sci. Fenn.* **42**, 125 (1972).
15. D. Creed, *Photochem. Photobiol.* **39**, 577 (1984); G. H. Beaven and E. R. Holiday, *Adv. Protein. Chem.* **7**, 4348 (1952).
16. D. B. Boyd, *J. Am. Chem. Soc.* **94**, 8799 (1972).
17. R. P. Rava and T. G. Spiro, *Biochemistry* **24**, 1860 (1985).
18. M. Ludwig and S. A. Asher, to be published.
19. J. L. Murtaugh, C. R. Johnson and S. A. Asher, in preparation.